

Northwestern University:
 N.U.H.E.P. Report No. 1101
 December 3, 2002

A global test of factorization for nucleon-nucleon, γp and $\gamma\gamma$ scattering

Martin M. Block ^{*}

*Department of Physics and Astronomy,
 Northwestern University, Evanston, IL 60208*

Kyungsik Kang [†]

*Department of Physics,
 Brown University, Providence, RI 02912*

Abstract

In this note, we show that the factorization relation $\sigma_{nn}/\sigma_{\gamma p} = \sigma_{\gamma p}/\sigma_{\gamma\gamma}$, where the σ 's are the total cross sections and nn denotes the even portion of the pp and $\bar{p}p$ total cross section, is satisfied experimentally in the energy domain $8 \leq \sqrt{s} \leq 2000$ GeV. The pp , $\bar{p}p$, γp and $\gamma\gamma$ total cross section data and the ρ -values for pp and $\bar{p}p$ are fit globally (simultaneously) using real analytic amplitudes that give a cross section rising asymptotically as $\ln^2(s)$. Within experimental errors, we show that factorization is satisfied when we unfold the published $\gamma\gamma$ data which averaged the cross sections obtained by using the two different PHOJET and PYTHIA Monte Carlo results. Our analysis clearly favors the PHOJET results and suggests that the additive quark model, together with vector meson dominance, allows one to compute $\sigma_{\gamma p}$ and $\sigma_{\gamma\gamma}$ from σ_{nn} with essentially no free parameters. The universal ρ -value, $\rho_{nn} = \rho_{\gamma p} = \rho_{\gamma\gamma}$, predicted by our fit, is compared to the ρ -value obtained by a QCD-inspired analysis of $\bar{p}p$ and pp data, including the p -air cross sections from cosmic rays. The ρ -values obtained from the two techniques are essentially indistinguishable in the energy region $8 \leq \sqrt{s} \leq 2000$ GeV.

^{*}Work partially supported by Department of Energy contract DA-AC02-76-Er02289 Task D.

[†]Work partially supported by Department of Energy contract DE-FG02-91-Er40688 Task A.

The purpose of this note is to investigate experimentally the factorization relation

$$\frac{\sigma_{nn}(s)}{\sigma_{\gamma p}(s)} = \frac{\sigma_{\gamma p}(s)}{\sigma_{\gamma\gamma}(s)}, \quad (1)$$

where the σ 's are the total cross sections and σ_{nn} , the total nucleon-nucleon cross section, is the *even* (under crossing symmetry) cross section for pp and $\bar{p}p$ scattering. Block and Kaidalov[1] have proved the factorization relation of eq. (1) using eikons for $\gamma\gamma$, γp and the even portion of nucleon-nucleon scattering, by assuming that

$$\left(\frac{\sigma_{\text{elastic}}(s)}{\sigma_{\text{tot}}(s)} \right)_{\gamma\gamma} = \left(\frac{\sigma_{\text{elastic}}(s)}{\sigma_{\text{tot}}(s)} \right)_{\gamma p} = \left(\frac{\sigma_{\text{elastic}}(s)}{\sigma_{\text{tot}}(s)} \right)_{nn}, \quad \text{for all } s. \quad (2)$$

They have further shown that

$$\rho_{nn}(s) = \rho_{\gamma p}(s) = \rho_{\gamma\gamma}(s), \quad (3)$$

where ρ is the ratio of the real to the imaginary portion of the forward scattering amplitude. These theorems are exact, for *all* s (where \sqrt{s} is the c.m.s. energy), and survive exponentiation of the eikonal (see ref. [1]). The assumption of eq. (2) implies that all of the processes approach a black disk in the same way, a geometric idea which seems physically reasonable, *i.e.*, the same opacity for nn , γp , and $\gamma\gamma$ scattering in the eikonsals satisfying s-channel unitarity, in contrast to a t-channel formalism such as the Regge eikonal model. In the Regge approach, factorization breaks down, in general, for singularities other than a simple pole in the complex angular momentum plane. However, since the radius of interaction for the Pomeron exchange which determines an eikonal grows with energy as $R^2 = R_o^2 + \alpha'_P \ln(s/s_0)$ and the Pomeron slope α'_P is very small, it was argued by Block and Kaidalov[1] that the factorization relations Eq (1) were expected to be valid to a good accuracy, even in a Regge model. Indeed, one can give “factorization-like” relations for the residue-like constants associated with double or triple poles in the angular momentum plane from t-channel unitarity [see Cudell *et. al.*[7]], with certain extra provisos.

We show that the factorization relations are supported by the experimental data for pp , $\bar{p}p$, γp , and $\gamma\gamma$ total cross sections and the pp and $\bar{p}p$ ρ -values fitted to analytic amplitudes that give asymptotic $\ln^2 s$ rise for the total cross sections. Our analysis favors in particular the PHOJET Monte Carlo analysis of the $\gamma\gamma$ data.

The major differences between our analysis and one done by the COMPETE collaboration[2] is that, in order to test factorization,

- we fit $\bar{p}p$, pp , γp and $\gamma\gamma$ data *simultaneously*, assuming complete factorization using the *same* shape parameters, whereas they fit each reaction separately, using *different* shape parameters
- we fit *individually* the two $\sigma_{\gamma\gamma}$ sets of OPAL and L3 data that are obtained using the PHOJET and PYTHIA Monte Carlos and do not use their average, since the two sets have different shapes and normalizations.

We will find the the total cross sections σ_{nn} , $\sigma_{\gamma p}$ and $\sigma_{\gamma\gamma}$, along with the corresponding ρ -values, by employing real analytic amplitudes. This technique has a hallowed tradition,

being first proposed by Bourrely and Fischer[3] and utilized extensively by Kang[4] and more recently by Block and collaborators[5, 6] and the COMPETE collaboration[2] for pp and $\bar{p}p$ scattering, by Block[8] for the investigation of ρ in γp scattering, by Block and Pancheri[9] for calculating ρ in $\gamma\gamma$ scattering, as well as by the COMPETE group[2]. This work follows the procedures and conventions used by Block and Cahn[5]. The variable s is the square of the c.m. system energy, p is the laboratory momentum and E is the laboratory energy. We will use a scattering amplitude that gives a total cross section that rises as $\ln^2(s)$. In terms of the even and odd forward scattering amplitudes f^+ and f^- (even and odd under the interchange of $E \rightarrow -E$), the even and odd total cross sections σ_{even} and σ_{odd} are given by the optical theorem as

$$\sigma_+ = \frac{4\pi}{p} \text{Im} f^+ \quad (4)$$

and

$$\sigma_- = \frac{4\pi}{p} \text{Im} f^-. \quad (5)$$

Thus,

$$\sigma_{\bar{p}p} = \sigma_+ + \sigma_- \quad (6)$$

and

$$\sigma_{pp} = \sigma_+ - \sigma_-. \quad (7)$$

The cross section σ_{nn} , referred to in the factorization theorem of eq. (1), is given by

$$\sigma_{nn} = \frac{4\pi}{p} \text{Im} f^+, \quad (8)$$

i.e., the *even* cross section. The unpolarized total cross sections for γp and $\gamma\gamma$ scattering are, in turn, given by

$$\sigma_{\gamma p} = \frac{4\pi}{p} \text{Im} f_{\gamma p}^+ \quad (9)$$

and

$$\sigma_{\gamma\gamma} = \frac{4\pi}{p} \text{Im} f_{\gamma\gamma}^-. \quad (10)$$

In all of the above, the f 's and σ 's are functions of s .

We further assume that our amplitudes are real analytic functions with a simple cut structure[5]. We will work in the high energy region, far above any cuts, (see ref.[5], p. 587, eq. (5.5a), with $a = 0$), where the amplitudes simplify considerably and are given by

$$\frac{4\pi}{p} f^+(s) = i \left\{ A + \beta [\ln(s/s_0) - i\pi/2]^2 + cs^{\mu-1} e^{i\pi(1-\mu)/2} \right\}, \quad (11)$$

and

$$\frac{4\pi}{p} f^-(s) = -Ds^{\alpha-1} e^{i\pi(1-\alpha)/2}, \quad (12)$$

where A , β , c , s_0 , D , μ and α are real constants. We are ignoring any real subtraction constants. In eq. (11), we have assumed that the nucleon-nucleon cross section rises asymptotically as $\ln^2 s$. Using equations (6) and (7), along with eq. (11) and eq. (12), the total cross sections $\sigma_{\bar{p}p}$, σ_{pp} and σ_{nn} for high energy scattering are given by

$$\sigma_{\bar{p}p}(s) = A + \beta \left[\ln^2 s/s_0 - \frac{\pi^2}{4} \right] + c \sin(\pi\mu/2)s^{\mu-1} - D \cos(\pi\alpha/2)s^{\alpha-1}, \quad (13)$$

$$\sigma_{pp}(s) = A + \beta \left[\ln^2 s/s_0 - \frac{\pi^2}{4} \right] + c \sin(\pi\mu/2)s^{\mu-1} + D \cos(\pi\alpha/2)s^{\alpha-1}, \quad (14)$$

$$\sigma_{nn}(s) = A + \beta \left[\ln^2 s/s_0 - \frac{\pi^2}{4} \right] + c \sin(\pi\mu/2)s^{\mu-1}, \quad (15)$$

and the ρ 's, the ratio of the real to the imaginary portions of the forward scattering amplitudes, are given by

$$\rho_{\bar{p}p}(s) = \frac{\beta \pi \ln s/s_0 - c \cos(\pi\mu/2)s^{\mu-1} - D \sin(\pi\alpha/2)s^{\alpha-1}}{\sigma_{\bar{p}p}}, \quad (16)$$

$$\rho_{pp}(s) = \frac{\beta \pi \ln s/s_0 - c \cos(\pi\mu/2)s^{\mu-1} + D \sin(\pi\alpha/2)s^{\alpha-1}}{\sigma_{pp}}, \quad (17)$$

$$\rho_{nn}(s) = \frac{\beta \pi \ln s/s_0 - c \cos(\pi\mu/2)s^{\mu-1}}{\sigma_{nn}}. \quad (18)$$

If we assume that the term in c is a Regge descending term, then $\mu = 1/2$.

To test the factorization theorem of eq. (1), we write the (even) amplitudes $f_{\gamma p}$ and $f_{\gamma\gamma}$ as

$$\frac{4\pi}{p} f_{\gamma p}(s) = iN \left\{ A + \beta[\ln(s/s_0) - i\pi/2]^2 + cs^{\mu-1}e^{i\pi(1-\mu)/2} \right\}, \quad (19)$$

and

$$\frac{4\pi}{p} f_{\gamma\gamma}(s) = iN^2 \left\{ A + \beta[\ln(s/s_0) - i\pi/2]^2 + cs^{\mu-1}e^{i\pi(1-\mu)/2} \right\}, \quad (20)$$

where N is the proportionality constant in the factorization relation $\frac{\sigma_{nn}(s)}{\sigma_{\gamma p}(s)} = \frac{\sigma_{\gamma p}(s)}{\sigma_{\gamma\gamma}(s)} = N$. We note, from eq. (11), eq. (19) and eq. (20), that

$$\rho_{nn} = \rho_{\gamma p} = \rho_{\gamma\gamma} = \frac{\beta \pi \ln s/s_0 - c \cos(\pi\mu/2)s^{\mu-1}}{A + \beta \left(\ln^2 s/s_0 - \frac{\pi^2}{4} \right) + c \sin(\pi\mu/2)s^{\mu-1}}, \quad (21)$$

thus satisfying the Block and Kaidalov[1] relation of eq. (3).

In the additive quark model, using vector dominance, the proportionality constant $N = \frac{2}{3}P_{\text{had}}^\gamma$, where P_{had}^γ is the probability that a photon turns into a vector hadron. Using (see Table XXXV, p.393 of Ref. [10]) $\frac{f_\rho^2}{4\pi} = 2.2$, $\frac{f_\omega^2}{4\pi} = 23.6$ and $\frac{f_\phi^2}{4\pi} = 18.4$, we find

$$P_{\text{had}}^\gamma \approx \Sigma_V \frac{4\pi\alpha}{f_V^2} = 1/249, \quad (22)$$

where $V = \rho, \omega, \phi$. In this estimate, we have neither taken into account the continuum vector channels nor the running of the electromagnetic coupling constant, effects that will tend to increase P_{had}^γ by several percent as well as give it a very slow energy dependence, increasing as we go to higher energies. In the spirit of the additive quark model and vector dominance, we now write

$$\sigma_{\gamma p}(s) = \frac{2}{3} P_{\text{had}}^\gamma \left(A + \beta \left[\ln^2 s/s_0 - \frac{\pi^2}{4} \right] + c \sin(\pi\mu/2) s^{\mu-1} \right) \quad (23)$$

and

$$\sigma_{\gamma\gamma}(s) = \left(\frac{2}{3} P_{\text{had}}^\gamma \right)^2 \left(A + \beta \left[\ln^2 s/s_0 - \frac{\pi^2}{4} \right] + c \sin(\pi\mu/2) s^{\mu-1} \right) \quad (24)$$

with the real constants A, β, s_0, c, D and P_{had}^γ (assuming $\alpha = \mu = 1/2$) being fitted by experiment. One might choose to vary the Regge intercepts μ and α in the fits. Since we want to test the goodness of the cross section factorization relations, we need a reasonable rendition of the *even* hadronic amplitude, *i.e.*, α plays *no* role. Further, a small deviation of μ from $1/2$ also gives no significant difference to our fit to shape of the hadronic data. Total cross sections for $\gamma\gamma$ scattering are now available for c.m.s. energies up to ≈ 130 GeV.

In making the fit, one is tempted to use the $\gamma\gamma$ cross sections, along with their errors, that are given in the Particle Data Group[11]. However, on closer inspection of the original papers, it turns out that results quoted by the PDG are the *averages of two independent* analyses performed by both the OPAL[13] and L3[12] groups, using the two different Monte Carlo programs, PHOJET and PYTHIA. The dominant error quoted was half the difference between the two different values.

The Monte Carlo simulations play a critical role in unfolding the $\gamma\gamma$ cross sections from the raw data. To quote the OPAL authors[13], “In most of the distributions, both Monte Carlo models describe the data equally well and there is no reason for preferring one model over the other for the unfolding of the data. We therefore average the results of the unfolding. The difference between this cross section and the results obtained by using PYTHIA or PHOJET alone are taken as the systematic error due to the Monte Carlo model dependence of the unfolding.” For the testing of factorization, there is good reason for possibly preferring one model over another, since the two models give both *different normalizations* and *shapes*, which are vital to our analysis. Hence, we have gone back to the original papers[12, 13] and have deconvoluted the data, according to whether PHOJET or PYTHIA was used. These results are given in Fig. 1. Clearly, there are major differences in shape and normalization that are due to the different Monte Carlos, with the PYTHIA results significantly higher and rising faster for energies above ≈ 15 GeV. However, the OPAL and L3 data seem to agree, within errors, for each of the two Monte Carlos, and thus, seem to be consistent with each other.

We will make three different fits, whose results are shown in Table 1. Fit 1 is a simultaneous χ^2 fit of eq. (13), (14), (16), (17) and (23) to the the experimental $\sigma_{\bar{p}p}$, σ_{pp} , $\rho_{\bar{p}p}$, ρ_{pp} and $\sigma_{\gamma p}$ data in the c.m.s. energy interval $10 \text{ GeV} \leq \sqrt{s} \leq 1800 \text{ GeV}$. We have also made simultaneous χ^2 fits of eq. (13), (14), (16), (17), (23) and (24) to the the experimental $\sigma_{\bar{p}p}$, σ_{pp} , $\rho_{\bar{p}p}$, ρ_{pp} , $\sigma_{\gamma p}$ and the *unfolded* $\sigma_{\gamma\gamma}$ (using either PHOJET or PYTHIA in our fit) data in the c.m.s. energy interval $10 \text{ GeV} \leq \sqrt{s} \leq 1800 \text{ GeV}$. Fit 2 uses $\sigma_{\gamma\gamma}$ from PHOJET

unfolding and Fit 3 uses $\sigma_{\gamma\gamma}$ from PYTHIA unfolding. In order to account for possible systematic normalization factors, the experimental cross sections for L3 are multiplied by the renormalization factor N_{L3} and those for OPAL are multiplied by the renormalization factor N_{OPAL} . These factors are also fitted in Fits 2 and 3.

From Fits 1, 2 and 3, we see that the major fit parameters A , β , s_0 , D , c and P_{had}^{γ} are the same, within errors. The purpose of Fit 1 was to show the robustness of our procedure, independent of the $\gamma\gamma$ data.

However, when we introduce the unfolded $\gamma\gamma$ cross sections in Fits 2 and 3, we see that the results strongly favor the PHOJET data of Fit 2. The $\chi^2/\text{d.f.}$ jumps from 1.49 to 1.87 (the total χ^2 changes from 115.9 to 146.0 for the same number of degrees of freedom). Further, and perhaps more compelling, the normalizations for both OPAL and L3 are in complete agreement, being 0.929 ± 0.037 and 0.929 ± 0.025 , respectively. Thus, they differ from unity by $\approx 7 \pm 3\%$, well within the experimental systematic normalization error of 5% quoted by L3. The PYTHIA results from Fit 3 have normalizations that disagree by $\approx 14\%$ and $\approx 19\%$ for OPAL and L3, respectively, in sharp disagreement with the 5% estimate. Thus, from here on, we only utilize the PHOJET results of Fit 2.

Using the parameters of Fit 2, we find that $P_{\text{had}}^{\gamma} = 1/(233.1 \pm 0.63)$, which is in reasonable agreement with our preliminary estimate of $1/249$, being $\approx 6\%$ larger, an effect easily accounted for by continuum vector channels in γp reactions that are not accounted for in the estimate of eq. (22).

The fitted total cross sections $\sigma_{\bar{p}p}$ and σ_{pp} from eq. (13) and eq. (14) are shown in Fig. 2, along with the experimental data. The fitted ρ -values, $\rho_{\bar{p}p}$ and ρ_{pp} from eq. (16) and eq. (17) are shown in Fig. 3, along with the experimental data. The fitted total cross section $\sigma_{\gamma p} = \frac{2}{3}P_{\text{had}}^{\gamma}\sigma_{nn}$ from eq. (23) is compared to the experimental data in Fig. 4, using $P_{\text{had}}^{\gamma} = 1/233$. The fitted total cross section $\sigma_{\gamma\gamma} = (\frac{2}{3}P_{\text{had}}^{\gamma})^2\sigma_{nn}$ from eq. (24) is compared to the experimental data in Fig. 5, again using $P_{\text{had}}^{\gamma} = 1/233$. The data plotted in Fig. 5 are *not* renormalized, but are the results of unfolding the original experimental results, *i.e.*, use $N_{OPAL} = N_{L3} = 1$. We see from Fig. 5 that within errors, both the *shape* and *normalization* of the PHOJET unfolding of both OPAL and L3 are in reasonable agreement with the factorization theorem of eq. (1), whereas the PYTHIA unfolding is in distinct disagreement.

The fitted results for $\sigma_{\gamma\gamma}$ are compared to the renormalized OPAL and L3 (PHOJET only) data in Fig. 6. The agreement in shape and magnitude is quite satisfactory, indicating strongly that factorization works.

For completeness, we show in Fig. 7 the expected ρ -value for the even amplitude, from eq. (21). Also shown in this graph is the predicted value for ρ_{nn} found from a QCD-inspired eikonal fit by Block *et al.*[14] to $\bar{p}p$ and pp total cross sections and ρ -values from accelerators plus p-air cross sections from cosmic rays. The agreement between these two independent analyses using

- real analytic amplitudes with a $\ln s^2$ behavior
- a QCD-inspired eikonal model in impact parameter space, giving rise to a cross section also eventually rising as $\ln s^2$,

is most striking.

We conclude that the factorization hypothesis of [1] is satisfied for nn, γp and $\gamma\gamma$ scattering, if one uses the PHOJET Monte Carlo program to analyze $\sigma_{\gamma\gamma}$ (and *not* the PYTHIA program). In particular, the data also satisfy the additive quark model using vector meson dominance, since

$$\begin{aligned}\sigma_{\gamma p} &= \frac{2}{3} P_{\text{had}}^{\gamma} \sigma_{nn} \\ \sigma_{\gamma\gamma} &= \left(\frac{2}{3} P_{\text{had}}^{\gamma}\right)^2 \sigma_{nn}.\end{aligned}\quad (25)$$

The assumption of Block and Kaidalov[1] in eq. (2) that $\sigma_{\text{elastic}}(s)/\sigma_{\text{tot}}(s)$ is process-independent yields another factorization theorem[1]

$$\frac{B_{nn}(s)}{B_{\gamma p}(s)} = \frac{B_{\gamma p}(s)}{B_{\gamma\gamma}(s)}, \quad (26)$$

where the B 's are the nuclear slopes for elastic scattering (the logarithmic derivatives of the elastic scattering cross sections $d\sigma_{\text{elastic}}/dt$, where t is the squared 4-momentum transfer). For γp processes, using vector dominance, the B 's are the slopes of the 'elastic' scattering reactions

$$\gamma + p \rightarrow V + p, \quad (27)$$

where the vector meson V is either a ρ , ω or ϕ meson. Using the additive quark model, eq. (26) implies that

$$B_{\gamma p}(s) = \kappa B_{nn}(s), \quad \text{where } \kappa = \frac{2}{3}. \quad (28)$$

It has been shown by Block, Halzen and Pancheri[15] that a χ^2 fit to the available γp data gives

$$\kappa = 0.661 \pm 0.008, \quad (29)$$

in excellent agreement with the $2/3$ value predicted by the additive quark model.

This reinforces our conclusion that after finding $\sigma_{nn}(s)$, ρ_{nn} and B_{nn} from experimental $\bar{p}p$ and $p\bar{p}$ data, we can then predict rather accurately $\sigma_{\gamma p}(s)$, $\rho_{\gamma p}$, $B_{\gamma p}$ and $\sigma_{\gamma\gamma}(s)$, $\rho_{\gamma\gamma}$, $B_{\gamma\gamma}$, using the additive quark model with vector dominance in essentially a *parameter-free* way. Clearly, this conclusion would be greatly strengthened by precision cross section measurements of both γp and $\gamma\gamma$ reactions at high energies.

Parameters	$\sigma_{\text{tot}} \sim \ln^2(s/s_0)$		
	Fit 1: no $\sigma_{\gamma\gamma}$	Fit 2: $\sigma_{\gamma\gamma}$ from PHOJET	Fit 3: $\sigma_{\gamma\gamma}$ from PYTHIA
A (mb)	37.2 ± 0.81	37.1 ± 0.87	37.3 ± 0.77
β (mb)	0.304 ± 0.023	0.302 ± 0.024	0.307 ± 0.022
s_0 ($(\text{GeV})^2$)	34.3 ± 14	32.6 ± 16	35.1 ± 14
D (mb(GeV) $^{2(1-\alpha)}$)	-35.1 ± 0.83	-35.1 ± 0.85	-35.4 ± 0.84
α	0.5	0.5	0.5
c (mb(GeV) $^{2(1-\mu)}$)	55.0 ± 7.5	55.9 ± 8.1	54.6 ± 7.3
μ	0.5	0.5	0.5
P_{had}^γ	$1/(233.1 \pm 0.63)$	$1/(233.1 \pm 0.63)$	$1/(233.0 \pm 0.63)$
N_{OPAL}	—	0.929 ± 0.037	0.861 ± 0.050
N_{L3}	—	0.929 ± 0.025	0.808 ± 0.020
$\chi^2/\text{d.f.}$	1.62	1.49	1.87
d.f.	68	78	78
total χ^2	110.5	115.9	146.0

Table 1: Fit 1 is the result of fit to total cross sections and ρ -values for $\bar{p}p$, pp and $\sigma_{\gamma p}$. Fit 2 and Fit 3 are the results of fitting total cross sections and ρ -values for $\bar{p}p$, pp and $\sigma_{\gamma p}$, along with the $\sigma_{\gamma\gamma}$ data from the OPAL and L3 collaborations. Fit 2 uses the results of unfolding $\sigma_{\gamma\gamma}$ with the PHOJET Monte Carlo, whereas Fit 3 uses the results of unfolding $\sigma_{\gamma\gamma}$ with the PYTHIA Monte Carlo. In both Fit 2 and Fit 3 the data renormalization factors N_{OPAL} and N_{L3} are also fitted. The parameters that are the results of the fit are the ones with statistical errors.

References

- [1] M. M. Block and A. B. Kaidalov, e-Print Archive: [hep-ph/0012365](https://arxiv.org/abs/hep-ph/0012365), Phys. Rev. D **64**, 076002 (2001).
- [2] J. R. Cudell *et al.*, Phys. Rev. D **65**, 074024 (2002); J. R. Cudell *et al.*, Phys. Rev. Lett. **89**, 201801 (2002).
- [3] C. Bourrely and J. Fischer, Nucl. Phys. B **61**, 513 (1973).
- [4] L. Lukaszuk and B. Nicolescu, Lett. Nuovo Cimento **8**, 405 (1973); K. Kang and B. Nicolescu, Phys. Rev. D **11**, 2461 (1975); G. Bialkowski, K. Kang and B. Nicolescu, Lett. Nuovo Cimento **13**, 401 (1975).

- [5] M. M. Block and R. N. Cahn, Rev. Mod. Phys. **57**, 563 (1985).
- [6] M. M. Block, K. Kang and A. R. White, Int. J. Mod. Phys. **A7**, 4449 (1992).
- [7] J. R. Cudell *et al.*, e-Print Archive: [hep-ph/0207196](#), [hep-ph/0209281](#) (2002).
- [8] M. M. Block, e-Print Archive: [hep-ph/0204048](#), Phys. Rev. D **65**, 116005 (2002).
- [9] M. M. Block and G. Panzeri, e-print Archive: [hep-ph/0206166](#), Eur. Phys. J. C **25** 287 (2002).
- [10] T. H. Bauer *et al.*, Rev. Mod. Phys. **50**, 261 (1978).
- [11] K. Hagiwara *et al.*, Phys. Rev. D, **66**, 010001 (2002).
- [12] L3 Collaboration, M. Acciarri *et al.*, Phys. Lett. **bf B519**, 33 (2001).
- [13] OPAL Collaboration, G. Abbiendi *et al.*, Eur. Phys. J. **C14**, 199 (2000).
- [14] M. M. Block *et al.*, e-Print Archive: [hep-ph/0004232](#), Phys. Rev. D **62**, 077501 (2000).
- [15] M. M. Block *et al.*, e-Print Archive: [hep-ph/0111046 v2](#), Eur. Phys. J. C **23**, 329 (2002).

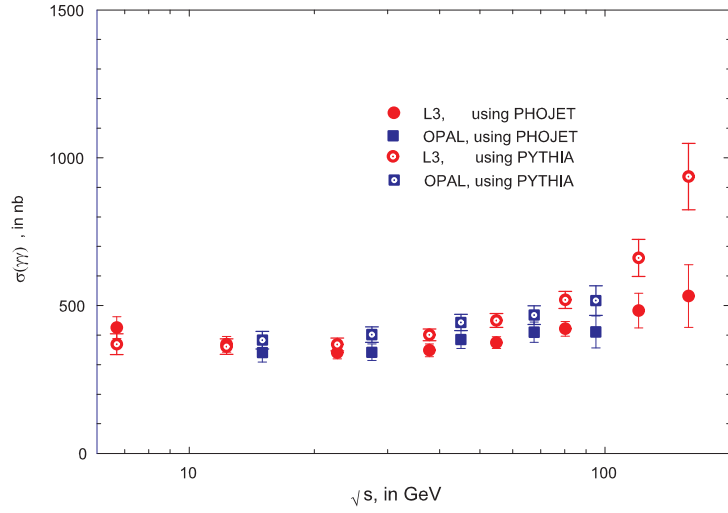


Figure 1: OPAL and L3 total cross sections for $\gamma\gamma$ scattering, in nb *vs.* \sqrt{s} , the cms energy, in GeV. The data have been unfolded according to the Monte Carlo used. The solid circles are the L3 data, unfolded using PHOJET and the open circles are the L3 data, unfolded using PYTHIA. The solid squares are the OPAL data, unfolded using PHOJET and the open squares are the OPAL data unfolded using PYTHIA.

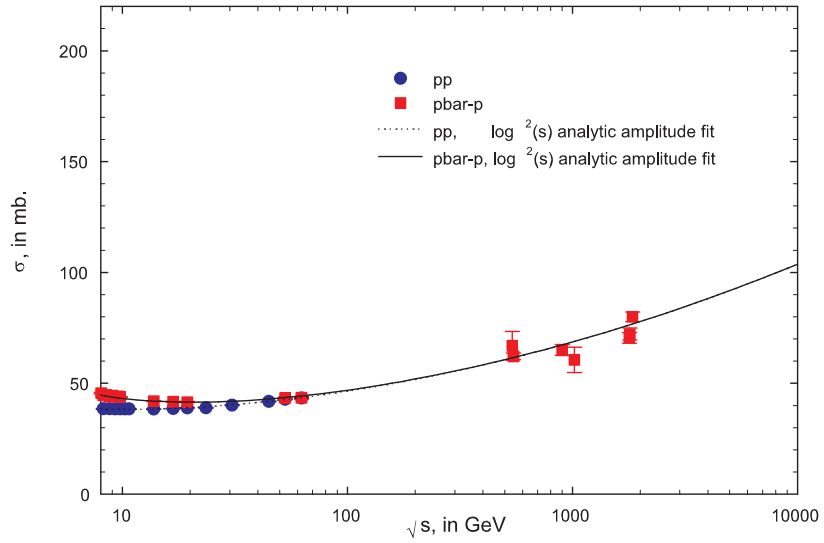


Figure 2: The dotted curve is σ_{pp} , the predicted total cross section for pp reactions, in mb, and the solid curve is $\sigma_{\bar{p}p}$, the predicted cross section for $\bar{p}p$ reactions, in mb *vs.* \sqrt{s} , the cms energy, in GeV. The circles are the experimental data for pp reactions and the squares are the experimental $\bar{p}p$ data.

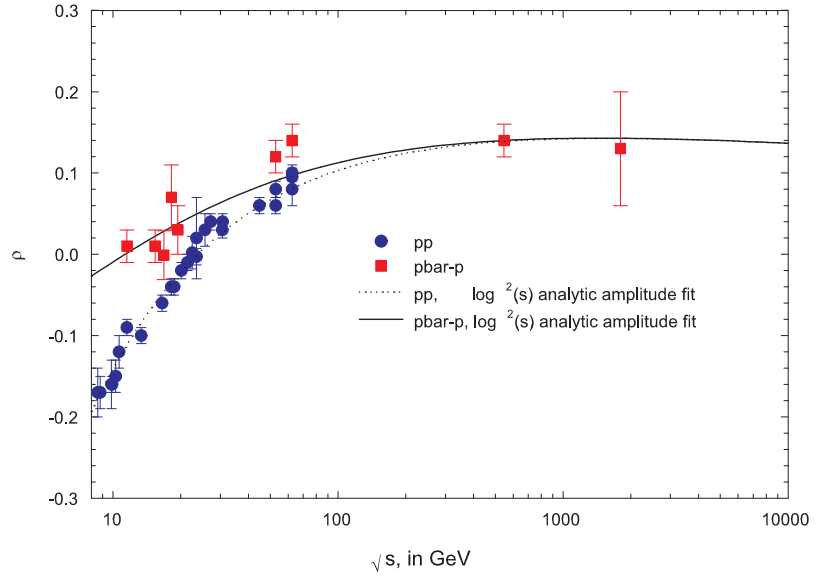


Figure 3: The dotted curve is ρ_{pp} , the predicted ratio of the real to imaginary part of the forward scattering amplitude for pp reactions and the solid curve is $\rho_{\bar{p}p}$, the predicted ratio for $\bar{p}p$ reactions, *vs.* \sqrt{s} , the cms energy, in GeV. The circles are the experimental data for pp reactions and the squares are the experimental $\bar{p}p$ data.

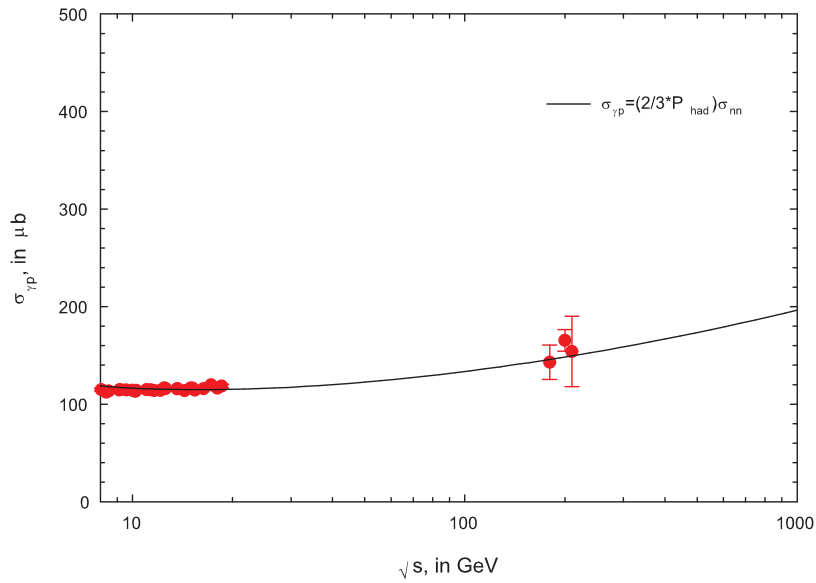


Figure 4: The curve is $\sigma_{\gamma p} = \frac{2}{3} P_{\text{had}}^{\gamma} \sigma_{nn}$, the predicted total cross section for γp reactions, in μb *vs.* \sqrt{s} , the cms energy, in GeV. The circles are the experimental data.

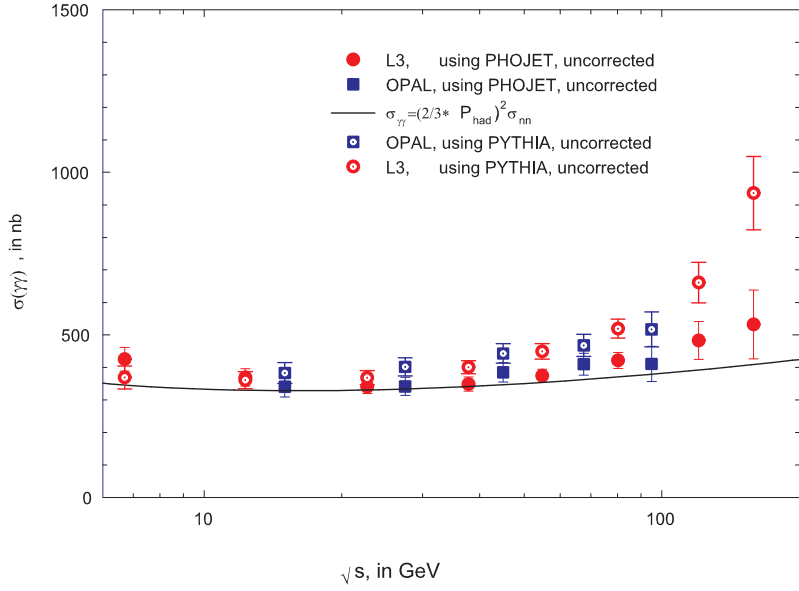


Figure 5: The curve is $\sigma_{\gamma\gamma} = \left(\frac{2}{3}P_{\text{had}}^{\gamma}\right)^2 \sigma_{\text{nn}}$, the predicted total cross section for $\gamma\gamma$ reactions, in nb, vs. \sqrt{s} , the cms energy, in GeV. The open squares and circles are the experimental total cross sections for OPAL and L3, respectively, unfolded using PYTHIA. The solid squares and circles are the experimental total cross sections for OPAL and L3, respectively, unfolded using PHOJET.

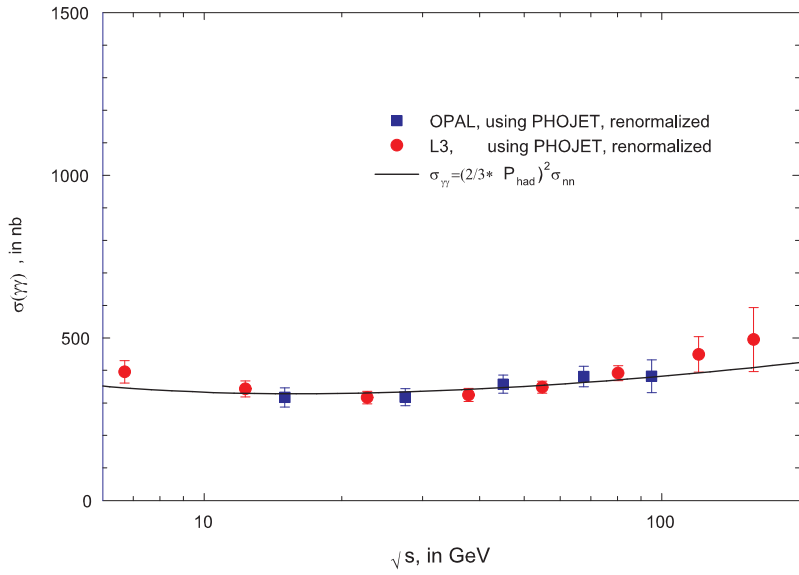


Figure 6: The curve is $\sigma_{\gamma\gamma} = \left(\frac{2}{3}P_{\text{had}}^{\gamma}\right)^2 \sigma_{\text{nn}}$, the predicted total cross section for $\gamma\gamma$ reactions, in nb, vs. \sqrt{s} , the cms energy, in GeV. The squares and circles are the total cross sections for OPAL and L3, respectively, unfolded using PHOJET, after they have been renormalized by the factors $N_{\text{OPAL}} = 0.929$ and $N_{\text{L3}} = 0.929$ found in Fit 2 of Table 1.

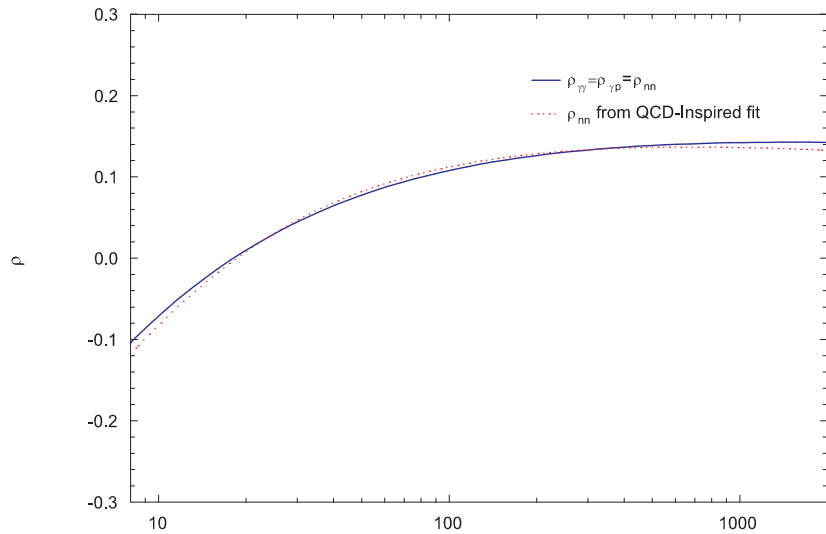


Figure 7: The solid curve is $\rho_{\gamma\gamma} = \rho_{\gamma p} = \rho_{nn}$, the predicted ratio of the real to imaginary part of the forward scattering amplitude for the even amplitude *vs.* \sqrt{s} , the cms energy, in GeV. The dotted curve, shown for comparison, is ρ_{nn} , the result of a QCD-inspired eikonal fit[14] to $\bar{p}p$ and $p p$ data that included cosmic ray p-air data.